OXFORD **Toxicology Research**

PAPER

Molecular docking analyses of CYP450 monooxygenases of *Tribolium castaneum* (Herbst) reveal synergism of quercetin with paraoxon and tetraethyl pyrophosphate: *in vivo and in silico studies*

Ammarah Ghaffar,[1,†] Sheikh Arslan Sehgal,[2,†] Rida Fatima,[1] Roya Batool,[1] Ume Aimen,[1] Sliha Awan,[1] Sajida Batool,[1] Faheem Ahmad (iD)[1,*] and Syed M. Nurulain[1,*]

[1]Department of Biosciences, COMSATS University Islamabad, Park Road, Tarlai Kalan, Islamabad 45550, Pakistan and [2]Department of Bioinformatics and Biotechnology, Government College University Faisalabad, Kotwali Rd, Gurunanakpura, Faisalabad 38000, Pakistan

*Correspondence address. Department of Biosciences, COMSATS University Islamabad, Park Road, Tarlai Kalan, Islamabad 45550, Pakistan. Phone: +923315874560; E-mail: faheem.ahmad@comsats.edu.pk; E-mail: syed.nurulain@comsats.edu.pk
†Equally contributed.

Abstract

Pest management in stored grain industry is a global issue due to the development of insecticide resistance in stored grain insect pests. Excessive use of insecticides at higher doses poses a serious threat of food contamination and residual toxicity for grain consumers. Since the development of new pesticide incurs heavy costs, identifying an effective synergist can provide a ready and economical tool for controlling resistant pest populations. Therefore, the synergistic property of quercetin with paraoxon and tetraethyl pyrophosphate has been evaluated against the larvae and adults of *Tribolium castaneum* (Herbst). Comparative molecular docking analyses were carried out to further identify the possible mechanism of synergism. It was observed that quercetin has no insecticidal when applied at the rate of 1.5 and 3.0 mg/g; however, a considerable synergism was observed when applied in combination with paraoxon. The comparative molecular docking analyses of CYP450 monooxygenase (CYP15A1, CYP6BR1, CYP6BK2, CYP6BK3) family were performed with quercetin, paraoxon and tetraethyl pyrophosphate which revealed considerable molecular interactions, predicting the inhibition of CYP450 isoenzyme by all three ligands. The study concludes that quercetin may be an effective synergist for organophosphate pesticides depending upon the dose and type of the compound. In addition, *in silico* analyses of the structurally diversified organophosphates can effectively differentiate the organophosphates which are synergistic with quercetin.

Key words: quercetin, phytochemical, synergism, molecular docking

Introduction

During grain storage, up to a quarter of the world grain reserves are lost due to insect infestation annually. Globally, several insecticides alongside fumigants are being used, but incidences of pesticide resistance development against those chemical protectants have been reported regularly [1, 2]. For the stored grain pests, phosphine is used widely as a fumigant, although strong resistance to phosphine has been reported in a number of stored grain pests including *Tribolium castaneum* [3]. Other than fumigation, organophosphate compounds (OPs) have been used as structural pest management [4]. There are more than 100 different kinds of organophosphates classified on the basis of their structures and functions [5] and also exhibit toxicity contrarily. Since most of the stored grain pests have developed resistance against these pesticides, they are needed to applied at higher concentration. This in turn exhibits occupational health hazards and possible residual contamination in the food chain [6]. Generally, for every 3 years of an organophosphate pesticide application, stored grain pests used to develop resistance against those pesticides. The range of chemicals that can be used safely having least environmental contamination as well as economically feasible to apply on grains is very limited.

One mechanistic approach is to add a synergist compound with the insecticide that can reduce the metabolism of pesticide in the body of the insects. With this objective, different plant metabolites and extracts have been evaluated for their insecticidal, repellent or synergistic properties [7]. *Tribolium castaneum*, the red flour beetle, attacks a wide range of human stored food and causes considerable damages [8]. The stored grain products including flour, cereals, crackers, beans, spices, pasta, cake mix, dried pet food, chocolate, nuts, seeds and even dried museum specimens are being attacked by the red flour beetle [8]. Although several natural compounds having synergistic activity against insect's CYP450 have been widely reported [9–11], a limited information is available regarding the activity of QCT on organophosphate detoxification mechanism in insect pests. The present study was designed to investigate the insecticidal potential in quercetin (QCT) and compare with two structurally different organophosphates, paraoxon (POX) and tetraethyl pyrophosphate (TEPP) against fifth instar larvae and adults of *T. castaneum*.

QCT is widely abundant in nature and is present in numerous fruits, vegetables, leaves and grains. Its tremendous medicinal value has been documented in literature [12–14]. In addition, its protective effect against organophosphate-induced toxicity in human has also been reported [15]. However, its insecticidal activity is less addressed, though it has been reported as constituents of extracts investigated for insecticidal value [16] against *Sitophilus zeamais* [17, 18] and *Helicoverpa armigera* [19] and even against the organophosphate resistant mites [20].

QCT has been reported to modulate CYP450 enzymes [21] and is an active inhibitor of several isoenzyme of CYP450 in vertebrates [22–24]. CYP450 monooxygenases not only detoxifies the organophosphate insecticides but also the QCT [25]; hence, mechanistically there could be a competitive effect by the combination of both QCT and organophosphate together resulting into the increased toxicity of organophosphate compounds. The study was designed with the assumption that QCT might act as synergist to organophosphates due to its reported esterase-inhibiting properties [26]. This will enable the reduction in dosage of environmentally hazardous chemical against resistant insect pests.

Furthermore, for the hit identification and lead optimization, comparative molecular docking analyses could give a broader view of the mechanism of synergism between QCT and organophosphate compounds. Bioinformatics helps to solve numerous biological problems [27] and have effective methodologies to design computer-aided drugs against cancer [28–31] and neurological disorders [32–35]. It has been reported that QCT has esterase-inhibiting properties [36]. Extensive literature review of QCT along with organophosphates compounds and CYP450 was the initial efforts of the current *in silico* analyses. The aims of the study were to evaluate the potential synergism effects of QCT with organophosphate pesticides used against *Tribolium castaneum* along with 3D structure prediction and evaluations of CYP15A1, CYP6BK2, CYP6BK3 and CYP6BR1 comparative molecular docking analyses with synergic effect to explore the molecular mechanism computationally. To attain our aims, the insect's culture, toxicity determination, synergic effects, threading and comparative modeling followed by the comparative molecular docking were applied. The following molecular docking methodology [37] had the potential to identify the molecular mechanism through computational biology. Finally, the outcome of this study may introduce a new insecticide complex with better efficacy than the existing standard pesticide and larvicide against resistant *T. castaneum*.

Materials and Methods

Insect culture

Insect cultures were sourced from stored product research laboratory in the University of Karachi and were reared in sterile jars containing wholemeal wheat flour mixed with yeast (10:1, w/w) at 32°C and 60% relative humidity with 14:10 hour's dark: light regime. All the bioassays were conducted on the fifth instar larvae and newly emerged adults of *T. castaneum* under the above mentioned laboratory condition.

Chemicals

QCT, a naturally occurring flavonoid in powdered form (Cat. No. 1592409), POX (Cat. No. PESTNATAL 36186) and TEPP (Cat. No. 32434.) were sourced from Sigma-Aldrich, USA. The minimized 2D structures of the selected ligands are presented in Fig. 1.

Insect bioassays

Toxicity determination. Toxicity bioassays of organophosphates and QCT against the fifth instar larvae and adult were carried out as described by [38]. Doses were optimized in preliminary pilot studies. The experiments were repeated thrice with three concentrations each for POX (0.055, 0.275 and 27.52 mg/g of diet) and TEPP (0.290, 1.451 and 29.019 mg/g of diet), and two doses of QCT (1.5 and 3.0 mg/g of diet) were used along with three control groups with diet treated with water, solvent or none (dry flour). Since no mortality was observed in any of the control treatment, the data is not mentioned.

Ten larvae or adults of uniform age were released in a Petri dish (90 × 15 mm) containing the treated diet or the controlled diet, accordingly. Daily data for insect mortality was recorded for 10 consecutive days. The data were analyzed statistically, and the survival curves were generated using Kaplan–Meir survival analysis on 10 days data using SPSS statistical software.

Evaluation of synergistic effect. The synergistic effect of QCT with organophosphates was evaluated using the above mentioned doses of POX and TEPP in combination with QCT at 3.0 mg/g of
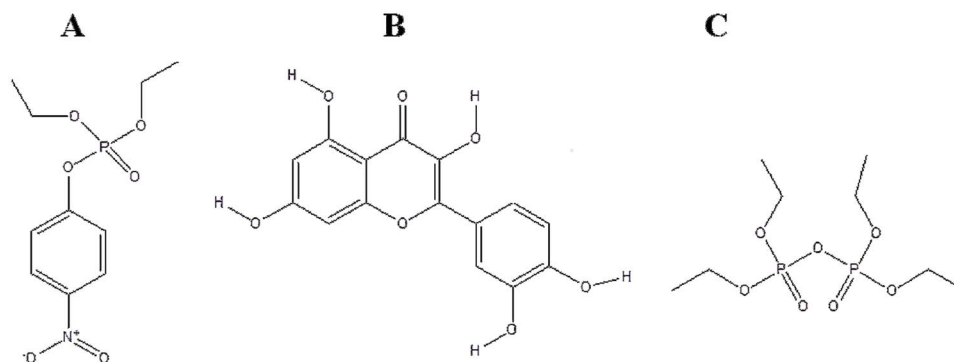
Figure 1: 2D structure of ligands under consideration. (**A**) Paraoxon (POX), (**B**) quercetin (QCT), (**C**) tetraethyl pyrophosphate (TEPP)

diet. The data were analyzed statistically as mentioned in earlier section.

In silico analyses

Homology modeling, evaluation and refinement. For *in silico* analyses, comparative modeling, threading approach and comparative molecular docking studies were performed. The canonical sequences of CYP450 enzymes, CYP15A1 (492 residues), CYP6BR1 (494 residues), CYP6BK2 (512 residues) and CYP6BK3 (506 residues) were retrieved in FASTA format from UniProt Knowledgebase [39] having accession numbers A0A0F7R7X8, D7EJ99, D7EJA7 and D7EJA6, respectively. The amino acid sequences of the selected proteins were subjected to BLASTp search against Protein Data Bank (PDB) [40] for suitable template structures. The top-ranked structures (Supplementary Table 1) were selected as suitable templates to predict the three-dimensional (3D) structures of the selected proteins by using homology modeling approach. MODELLER 9v13 [41], an automated protein modeling program, was employed to predict the 3D structures of the selected proteins by satisfying the spatial restraints. Numerous online software including RaptorX [42], SWISS MODEL [43], M4T [44], I-TASSER [45] and Phyre2 [46] were utilized for structure prediction to predict the 3D models. The energy minimization followed by geometry optimization was done by using UCSF Chimera 1.8 [47] for 1000 steps (step size 0.02 Å), utilizing the conjugate gradient method followed by the protonation of wild-type histidines by employing the force field of AMBER ff98 method [48]. The evaluation tools including ERRAT [49], Procheck [50] and verify3D [51] were applied to evaluate the quality of the predicted CYP26A1 model. The predicted 3D models were further assessed by MolProbity [52] server. Finally, the poor rotamers and ramachandran outliers were corrected by using WinCoot [53] tool.

PROCHECK evaluates the 3D positioning of each atom and residues of the protein structure, while ERRAT analyzes the statistics of nonbonded interactions between different atom types. Verify3D determines the compatibility of an atomic model (3D) with its own amino acid sequence (1D) [54, 55].

Molecular docking. Extensive literature review was performed to analyze the amino acid position of heme, and it was observed that CYPs bind with heme for efficient working. The Cys-436, Cys-438, Cys-457 and Cys-457 residues of CYP15A1, CYP6BR1, CYP6BK2 and CYP6BK3 were observed and selected for the heme binding, respectively. The blind and targeted dockings were performed by GOLD [56] and AutoDock Vina [57] docking software for the binding of heme against the selected proteins at appropriate positions. UCSF Chimera 1.13, Ligplot [58] and MoE [59] were used to analyze the molecular docking and interactions of heme.

Comparative molecular docking studies were done by AutoDock 4.2 tool, GOLD and AutoDock Vina [60]. The total 100 docking runs were set for each docking experiment, and polar atoms of hydrogen were added to the receptor proteins. The grid size for the docking studies was set at $65 \times 65 \times 65$ Å in X, Y and Z axes, respectively, with the grid spacing value of 0.710 Å to cover the whole receptor proteins and 0.450 Å for targeted docking at heme binding sites. The default parameters were used, while the genetic algorithm was used as the main searching protocol. The geometry optimization and energy minimization of the ligand compounds were done by using ChemDraw Ultra [61] and UCSF Chimera 1.6. The docked complexes were visualized and analyzed by employing ligplot, MoE, UCSF Chimera 1.8 and AutoDock 4.2 tools.

Results

Toxicity of paraoxon (POX)

The baseline toxicity of the POX was applied with or without QCT against *T. castaneum* (Tables 1 and 2). The application of POX demonstrated a dose-dependent mortality of larvae and the adults. The first day of applying the dose did not kill the larvae, while the highest dose of POX was applied (Table 1); however, on the second day after application, 66.7% of the larvae were killed in the same dose treatment (27.52 mg/g). Later, on the fifth day after application, the mortality in this treatment topped to at 100% (Table 1). In contrast, the lowest dose of POX (0.055 mg/g) did not produce any mortality. Similar results were observed for the toxicity test of POX against adult beetles, except with the treatment of POX at 27.52 mg/g—73.3% beetles got killed after 1 day (Table 1).

The only dose of QCT was applied at the rate of 3.0 mg/g of diet, and no mortality fluctuation to both larvae and adults (Table 2) was observed. However, the combination of POX and QCT knocked down the effect of the treatment on the first and second day after application (Table 2). The 20% of the increased mortality was observed with the combination of POX (0.275 mg/g) and QCT (3.0 mg/g) against larvae and adults, while 10% increased mortality at the highest dose of POX was observed due to QCT synergism (Table 2), as compared to the POX only treatments (Table 1).

POX applied at the rate of 27.52 mg/g caused 73% mortality, even when it was applied individually (Table 1). In contrast, QCT increased this effect of POX and reached 90% mortality (Table 2), hence demonstrating significant synergism between POX and

Table 1: Toxicity of paraoxon (POX) against the fifth instar larvae of *Tribolium castaneum* and adult over time

Doses (mg/g)	Percent mortality				
	1st day	2nd day	5th day	6th day	10th day
Larval toxicity					
0.055	0	0	0	0	0
0.275	0	46.7 ± 3.3	83.3 ± 16.7	100.0 ± 0.0	100.0 ± 0.0
		(32.3–61.0)	(11.6–155.0)	—	—
27.52	20.0 ± 05.8	66.7 ± 12.0	100.0 ± 0.0	100.0 ± 0.0	100.0 ± 0.0
	(0.0–44.8)	(14.9–118.3)	—	—	—
Adult toxicity					
0.055	0	0	0	0	0
0.275	0	46.7 ± 3.3	83.3 ± 16.7	100.0 ± 0.0	100.0 ± 0.0
	—	(32.3–61.0)	(11.6–155.0)	—	—
27.52	73.3 ± 12.0	76.7 ± 08.8	86.7 ± 13.3	100.0 ± 0.0	100.0 ± 0.0
	(21.6–125.0)	(38.7–114.6)	(29.3–144.0)	—	—

The data is presented as percent mortality means ± SEM (first row). The second row shows the respective 95% confidence interval of the mean.

Table 2: Synergistic effects of quercetin (QCT) when used in combination with paraoxon (POX) against *Tribolium castaneum*

Doses (mg/g)	Percent mortality				
	1st day	2nd day	5th day	6th day	10th day
Larval toxicity					
QCT 3.0	0	0	0	0	0
POX 0.055 + QCT 3.0	0	3.3 ± 3.3	16.7 ± 12.0	30.0 ± 15.3	33.3 ± 14.5
		(0.0–17.7)	(0.0–68.7)	(0.0–95.7)	(0.0–95.8)
POX 0.275 + QCT 3.0	0	63.3 ± 6.7	80.0 ± 11.5	100.0 ± 0.0	100.0 ± 0.0
		(34.6–92.0)	(30.3–129.8)	—	—
POX 27.52 + QCT 3.0	0	73.3 ± 6.7	100.0 ± 0.0	100.0 ± 0.0	100.0 ± 0.0
		(44.6–102.0)	—	—	—
Adult toxicity					
QCT 3.0	0	0	0	0	0
POX 0.055 + QCT 3.0	0	0	0	0	0
POX 0.275 + QCT 3.0	0	63.3 ± 6.7	80.0 ± 11.5	100.0 ± 0.0	100.0 ± 0.0
		(34.6–92.0)	(30.3–129.8)	—	—
POX 27.52 + QCT 3.0	90.0 ± 05.8	90.0 ± 05.8	96.7 ± 03.3	100.0 ± 0.0	100.0 ± 0.0
	(65.2–114.8)	(65.2–114.8)	(82.3–111.0)		

The data is presented as percent mortality means ± SEM, while the values in parenthesis, below each mean, are the respective 95% confidence interval.

QCT. Similar pattern was observed by Kaplan–Meier survival curve generated using 10 days of mortality data (Fig. 2). QCT when used in mixture with POX increased POX toxicity, and this is clearly mentioned by a 50% decline in the LD_{50} values for POX.

Toxicity of tetraethyl pyrophosphate (TEPP)

The similar toxicity pattern of TEPP against *T. castaneum* was observed with or without QCT combination (Tables 3 and 4). The mortality of both the larvae were found to ne dose and time dependent; however, TEPP had relatively lesser toxicity compared to POX (Table 3). In general, the 0.29 mg/g dose of TEPP produced the highest mortality of *T. castaneum* larvae. All other treatments against the larvae and adults produced mortality that was less than 10% (Table 3). Furthermore, QCT did not have any synergistic effect on TEPP toxicity, except when applied against the larvae at the rate of 29.019 mg/g (Table 4).

In silico analyses

The initial efforts for *in silico* studies were based on the relation of CYP450 enzymes (CYP15A1, CYP6BR1, CYP6BK2 and CYP6BK3) with QCT, POX, TEPP and its computational analyses to identify the molecular mechanism along with heme and Fe. The 3D structures of the selected proteins were not reported by NMR and X-ray crystallography techniques yet. The threading approaches and comparative modeling techniques were employed to predict the 3D models of the selected proteins. The amino acid sequences of the selected receptor proteins were subjected to protein–protein BLAST against the PDB database to search the suitable templates. The suitable top-ranked optimally aligned templates belong from CYP family with E-value and query coverage were selected to perform the comparative modeling (Supplementary Table 1). The alignment of the protein sequences showed that the conserved sequence region will share similar structures and functions. The selected templates were used to predict the 3D structures of the selected proteins. The overall identity between the selected templates and the selected proteins showed >38% from end-to-end amino acid sequence that was not considered reliable for the satisfactory structure prediction by using the comparative modeling approach. Threading approach was employed for better 3D structure and to overcome the errors.

In silico approaches (comparative modeling and threading) were employed by satisfying the spatial constraints to predict 19
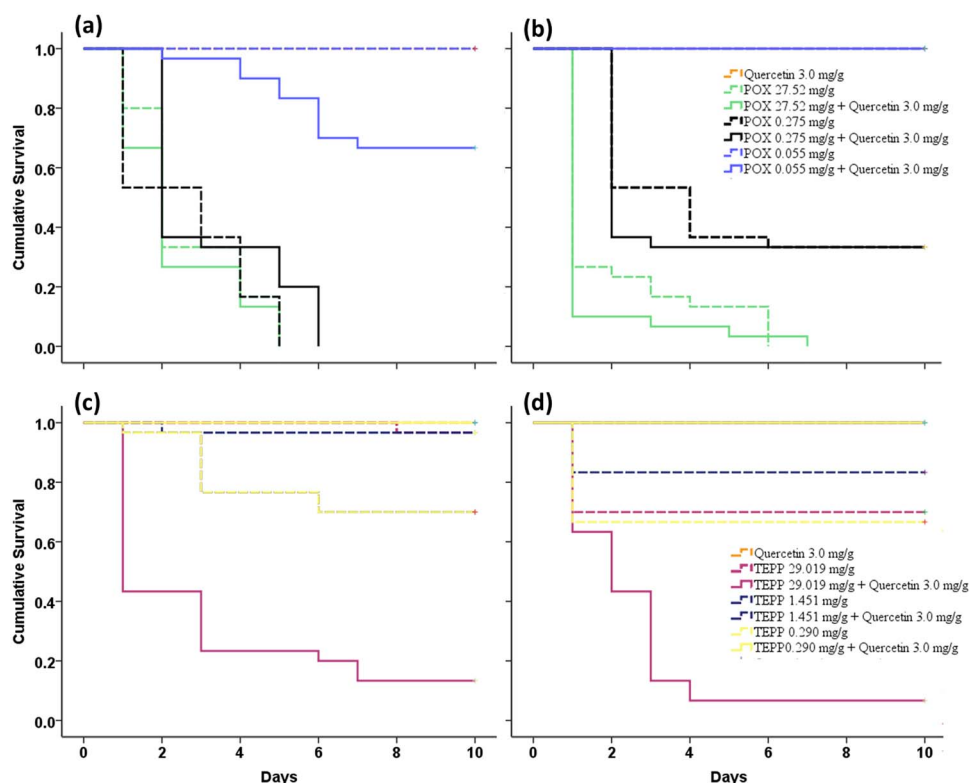
Figure 2: Kaplan–Meier survival curves generated for 10 days mortality data of POX (**a** and **b**) and TEPP (**c** and **d**) against *Tribolium castaneum* larvae (a and c) and adults (b and d). Synergistic effect of quercetin with POX is evident, as fewer insects survived when OP is co-applied with quercetin 3.0 mg/g (bottom line in graphs)

Table 3: Toxicity of tetraethyl pyrophosphate (TEPP) against the fifth instar larvae of *Tribolium castaneum* and adult over time

Doses (mg/g)	Percent mortality				
	1st day	2nd day	5th day	6th day	10th day
Larval toxicity					
0.290	3.3 ± 3.3	3.3 ± 3.3	23.3 ± 23.3	30.0 ± 30.0	± 30.0
	(0.0–17.7)	(0.0–17.7)	(0.0–123.7)	(0.0–159.0)	(0.0–159.0)
1.451	6.7 ± 6.7	6.67 ± 6.7	6.67 ± 6.7	6.7 ± 6.7)	6.7 ± 6.7
	(0.0–35.4)	(0.0–35.3)	(0–35.3)	(0.0–35.3)	(0.0–35.3)
29.019	0	0	0	0	3.3 ± 3.3
					(0.0–17.7)
Adult toxicity					
0.290	3.3 ± 3.3	3.3 ± 3.3	3.3 ± 3.3	3.3 ± 3.3	3.3 ± 3.3
	(0.0–17.7)	(0.0–17.7)	(0.0–17.7)	(0.0–17.7)	(0.0–17.7)
1.451	16.7 ± 8.8	3.3 ± 3.3	3.3 ± 3.3	3.3 ± 3.3	3.3 ± 3.3
	(0.0–54.6)	(0.0–17.7)	(0.0–17.7)	(0.0–17.7)	(0.0–17.7)
29.019	0	0	0	0	3.3 ± 3.3
					(0.0–17.7)

The data is presented as percent mortality means ± SEM (first row). The second row shows the respective 95% confidence interval of the mean.

structures for each protein by using various tools (MODELLER 9.14, Phrex2, SWISS MODEL, RaptorX, M4t and I-TASSER). All the predicted structures were evaluated on the basis of passing score, overall quality factor, favored region, outliers (Supplementary File 1) and heme binding region. Graphs were plotted (Supplementary Figs 1–16) by utilizing the evaluated values of all the generated models, and the most reliable structure was selected that favors the model generated from threading approach.

The ERRAT evaluation tool calculated the overall quality factor of 82.64, 89.09, 94.44 and 92.77% for the predicted structures of the CYP15A1, CYP6BR1, CYP6BK2 and CYP6BK3, respectively, depicting the high-quality structures. After critical examining, the predicted structures (Fig. 3) have the potential to be utilized for further analyses.

The reported protein structures of CYP family were retrieved from the PDB and also observed the heme binding site from literature [62–65]. It was observed that the heme and Fe bound at similar position in all the CYP family. The heme was docked against the selected proteins at the observed binding domain by using GOLD docking software. Interestingly, it was observed that the heme bound at the exact similar position counseling with the

Table 4: Synergistic effects of quercetin (QCT) when used in combination with tetraethyl pyrophosphate (TEPP) against *Tribolium castaneum*

Doses (mg/g)	Percent mortality				
	1st day	2nd day	5th day	6th day	10th day
Larval toxicity					
QCT 3.0	0	0	0	0	0
TEPP 0.290 + QCT 3.0	0	0	0	0	0
TEPP 1.451 + QCT 3.0	0	3.3 ± 3.3	3.3 ± 3.3	3.3 ± 3.3	3.3 ± 3.3
		(0.0–17.7)	(0.0–17.7)	(0.0–17.7)	(0.0–17.7)
TEPP 29.019 + QCT 3.0	56.7 ± 3.3	56.7 ± 3.3	76.7 ± 12.0	80.0 ± 11.5	86.7 ± 13.3
	(42.3–71.0)	(42.3–71.0)	(24.9–128.7)	(30.3–129.8)	(29.3–144.0)
Adult toxicity					
QCT 3.0	0	0	0	0	0
TEPP 0.290 + QCT 3.0	0	0	0	0	0
TEPP 1.451 + QCT 3.0	0	0	0	0	0
TEPP 29.019 + QCT 3.0	3.3 ± 3.3	3.3 ± 3.3	3.3 ± 3.3	3.3 ± 3.3	3.3 ± 3.3
	(11.0–17.7)	(11.0–17.7)	(11.0–17.7)	(11.0–17.7)	(11.0–17.7)

The data is presented as percent mortality means ± SEM, while the values in parenthesis, below each mean, are the respective 95% confidence interval.
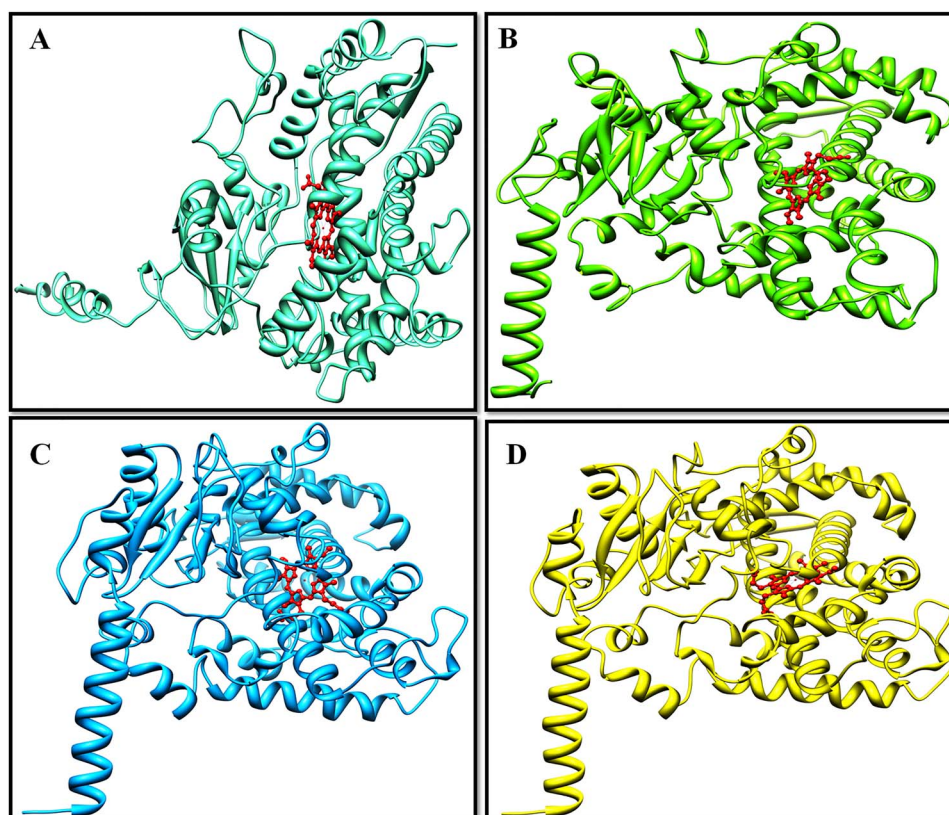

Figure 3: Pictorial representation of the binding residues identified via structure-based multiple sequence alignment (**a**) presents superimposition of the target and the template proteins (yellow color represents the target (CYP450) proteins, whereas brown color represents the template), (**b**) presents zoomed in view of the binding pocket with conserved residues labeled and (**c**) is the sequential representation of the structure-based alignment. The conserved residues in both target and the template are highlighted in green

other CYP protein family having the distance of <2.00 Å (Fig. 1). The selected inhibitors (Fig. 1) in the present analyses showed significance binding analyses of heme with CYP family.

However, the comparative molecular docking analyses of the selected inhibitors showed fluctuation in the observed binding energies, and the suitable docked complex having least binding energy was selected among all the generated docking complexes for each inhibitor. It was observed that the selected inhibitors showed effective binding against the selected proteins and heme. The molecular docking analyses were performed against the selected inhibitors by employing GOLD and also cross validate the molecular docking analyses by using AutoDock Vina and
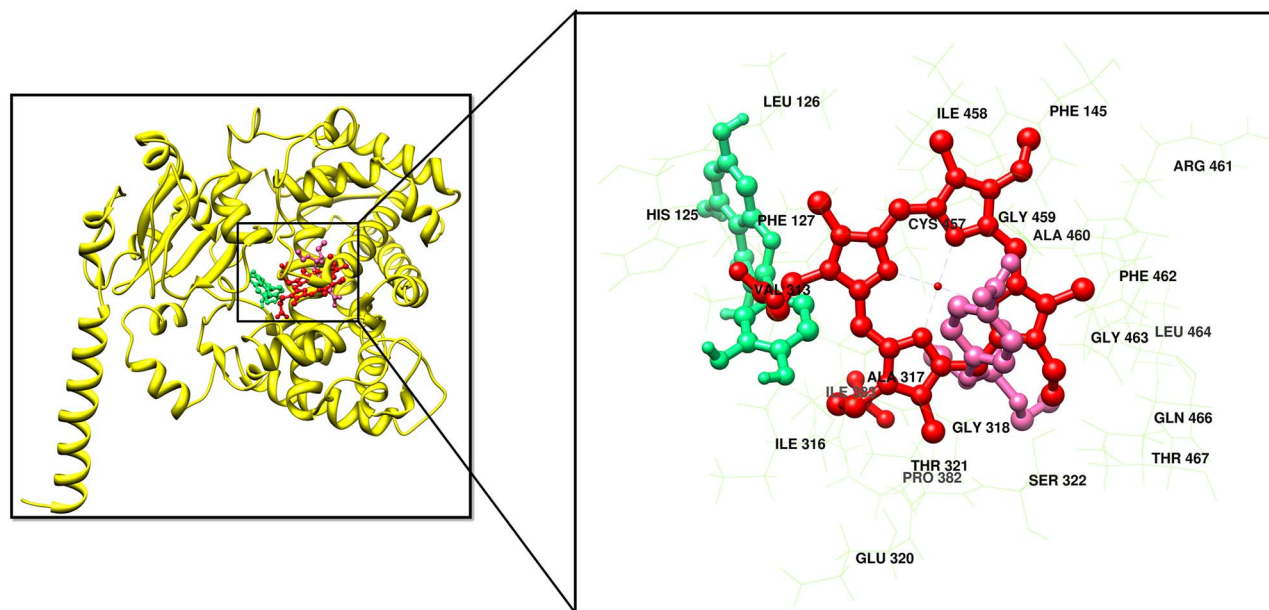
Figure 4: 3D representation of interactions among CYP450 proteins and respective ligands. The dark brown color represents the ligands, and light brown color represents the receptor. The hydrogen bond along with the distances is shown in green

AutoDock. All the docked complexes were ranked through highest binding affinity with heme and least binding energy. The top 5 docked complexes for each complex were analyzed critically. The blind and targeted docking analyses were performed for all the selected proteins to cross validate the results. Interestingly, it was observed that the compounds showed similar binding sites through both blind and targeted docking analyses. Extensive comparative molecular docking analyses revealed that QCT and POX showed least binding energy values and highest binding affinity with heme against CYP6BK3. The binding residues Leu-126, Phe-145, Ile-458, Arg-461, Gly-459, His-125, Phe-127, Cys-457, Ala-460, Phe-462, leu-464, Gly-463, Val-313, Ala-317, Ile-363, Gly-318, Thr-321, Pro-382, Ser-322, Thr-467 and Glu-320 of CYP6BK3 exhibited highest binding affinity against heme and selected molecules (Fig. 4).

Discussion

Our investigation revealed that the QCT alone is not an effective protecting agent against the adult and fifth instar larvae of flour beetle, but it possesses profound synergistic effect when mixed with POX. Although our findings warrant further investigation of the toxicity of QCT against insect pests, the inactivity of QCT is supported by earlier studies conducted against two other species of insects, i.e., larvae of *Helicoverpa armigera* and *Spodoptera litura* [66]. However [22] reported the deleterious effect of QCT to the third instar larvae of cotton boll worm, *Helicoverpa armigera* at higher doses only. Similarly, no previous studies could be traced on the understudied CYP450 isoenzymes. Moreover, it is evident from the literature that flavonoids inhibit esterases and monooxygenases, in general [67], and similarly QCT showed tissue- and dose-specific influence on the expression of CYP450 in *H. armigera* [22, 68] which found that *Mythimna separata* larvae had different metabolic strategies for QCT at different stages of the development. Flavonoids like QCT have medicinal value, and it has been reported as protecting agent to many pathological conditions [69, 70]. It can interfere with reproduction, molting

and feeding behavior of insects and their larvae [71]. The synergistic effect of QCT to profenofos, an organophosphate, against cotton leafworm has already been reported. [72–74] reported that the QCT has the potential to increase the mortality of first instar Colorado potato beetle larvae after 48 hours with the combination of Guthion, an organophosphate. Hence the frequently reported esterase-inhibiting nature of QCT might be considered as the mechanism of synergism reported in our studies.

Several *in vivo* and *in vitro* studies in human and mouse models have indicated that flavonoids may enhance or actively inhibit certain CYP450 isoenzyme. According to [75], CYP450 is distinctive to every species, and no organism shares identical CYP450. The CYP450 enzymes may be inhibited or induced, resulting in the modulation of physiological processes and toxicokinetics of xenobiotics. One of the reasons for insecticide resistance in insects has been attributed to the increased activities of CYP450 monooxygenases [76, 77], and mostly isozymes from family 6 has been implicated in conferring resistance in insect pests. For instance, susceptible strain of a mosquito *Aedes albopictus* exhibited 5-fold inhibition of CYP6P15 by an organophosphate temephos [77]. CYP6BK2 was reported to be increased in deltamethrin, a pyrethroid insecticide-resistant *T. castaneum* [78]. Vice versa, theoretically and mechanistically, decrease in CYP450 monooxygenases will increase the sensitivity of the insecticide.

Heme is considered as a vital cofactor, and the control of degradation and synthesis of heme are finely tuned by cellular contents. The excess of heme becomes toxic for the cells, while the deficiency leads to harm the cells [79]. Including CYP450, usually the cellular heme behaves as a functionally diverse hemoprotein prosthetic moiety [79]. The heme is the mandatory cofactor for the activity of the CYP450.

The observed results showed that the QCT was used in combination with POX; it resulted into knockdown effect as soon as 1 day after application, and 10–20% increase in larval and adult mortalities was observed due to QCT. The addition of QCT also had 1-fold increase in toxicity of POX, and LD_{50} was reduced to half the concentration required when POX was used alone. These synergistic results of QCT can be attributed to the ability

of QCT to inhibit the function of CYP450 protein in insects. Since CYP450 monooxygenases are among the main enzymes involved in insecticides resistance, the use of QCT can provide an efficient and effective resistance management strategy against *T. castaneum*. The present work, hence, focuses on four selected CYPs, all of which are present in *Tribolium* spp., where three of them, i.e., CYP6BR1, CYP6BK2 and CYP6BK3, are monooxygenases having established role in CYP-mediated insecticide resistance mechanisms [78], while the fourth (CYP15A1) is involved in embryogenesis [80].

In silico approaches including comparative modeling and comparative molecular docking were performed to further evaluate the role of QCT in modulating CYP450 proteins. The 3D structures of the selected CYP proteins were not reported by experimental techniques in PDB. The 3D structures of the selected proteins were predicted by utilizing the comparative modeling and threading approaches. The predicted models showed a good degree of accuracy, keeping in view the heme binding site of the selected proteins. Comparative molecular docking was performed by AutoDock Tools and GOLD, which leads to the synergic effects of QCT and POX against the mortality of larvae. Extensive comparative molecular docking analyses of the interactions among the combination of QCT and POX along with heme reconciled with the *in vitro* analyses. The observed results suggested that the highest binding affinity and least binding energy (Supplementary File 2) satisfy the accuracy of comparative molecular docking analyses [33, 35]. With the parameter satisfaction of least binding energy and coinciding with the statement of highest binding affinity against utilized ligands and heme, it is suggested that the synergic combination of QCT and POX against CYP6BK3 has a potential to affect the mortality of larvae. Our docking results revealed the involvement of Leu-126, Phe-145, Ile-458, Arg-461, gly-459, His-125, Phe-127, Cys-457, Ala-460, Phe-462, leu-464, Gly-463, Val-313, Ala-317, Ile-363, Gly-318, Thr-321, Pro-382, Ser-322, Thr-467 and Glu-320 residues for the interaction of heme, QCT and POX. CYP6BK3 protein from the current work had the lowest binding energy and highest binding affinity with heme, QCT and POX for synergic effect. It stands to the reason that the selected proteins and scrutinized protein (CYP6BK3) after extensive *in silico* molecular docking analyses has the potential to be an effective candidate for affect the mortality of the larvae.

Conclusion

It is concluded that QCT may be a good synergist to organophosphates. However, synergistic effect of QCT depends upon optimal doses and type of OPs. Based on molecular docking, it may be speculated that QCT and organophosphates decreased the activity of CYP450 enzymes, which in turn showed the enhanced larvicidal and adult toxicity. Furthermore, *in silico* molecular docking may be effectively applied to separate out the synergizeable organophosphates.

Supplementary data

Supplementary data is available at *TOXRES Journal* online.

Acknowledgements

Conflict of interest statement

The authors report no conflict of interest associated with this manuscript.

Credit statement

References

1. Moyes CL, Vontas J, Martins AJ *et al*. Contemporary status of insecticide resistance in the major Aedes vectors of arboviruses infecting humans. *PLoS Negl Trop Dis* 2017;**11**:e0005625.

2. Bass C, Denholm I, Williamson MS *et al*. The global status of insect resistance to neonicotinoid insecticides. *Pestic Biochem Physiol* 2015;**121**:78–87.

3. Cato AJ, Elliott B, Nayak MK *et al*. Geographic variation in phosphine resistance among north American populations of the red flour beetle (Coleoptera: Tenebrionidae). *J Econ Entomol* 2017;**110**:1359–65.

4. Chanbang Y, Arthur FH, Wilde GE *et al*. Subramanyam, methodology for assessing rice varieties for resistance to the lesser grain borer, *Rhyzopertha dominica*. *J Insect Sci* 2008;**8**:1–5.

5. Nurulain SM. Acute organophosphorus poisoning approaches for treatment. *Aust Dent J* 2013;**334**:134–47.

6. Wang Z, Zhao Z, Abou-Zaid MM *et al*. Inhibition of insect glutathione s-transferase (gst) by conifer extracts. *Arch Insect Biochem Physiol* 2014;**87**:234–49.

7. Mukherjee S, Joseph M. Medicinal plant extracts influence insect growth and reproduction: a case study. *J Med Aromat Plant Sci* 2000;**22**:154–8.

8. Weston PA, Rattlingourd PL. Progeny production by *Tribolium castaneum* (Coleoptera: Tenebrionidae) and *Oryzaephilus surinamensis* (Coleoptera: Silvanidae) on maize previously infested by *Sitotroga cerealella* (Lepidoptera: Gelechiidae). *J Econ Entomol* 2000;**93**:533–6.

9. Dai L, Ma M, Wang C *et al*. Cytochrome P450s from the Chinese white pine beetle, *Dendroctonus armandi* (Curculionidae: Scolytinae): expression profiles of different stages and responses to host allelochemicals. *Insect Biochem Mol Biol* 2015;**65**:35–46.

10. Fan Y, Kang Z, Wang Z *et al*. Quercetin and paraoxon induction of hydrolase activity in *Helicoverpa armigera* and malathion-susceptible and resistant *Musca domestica*. *Entomol Gen* 2018;**38**:157–71.

11. Tao X-Y, Xue X-Y, Huang Y-P *et al*. Gossypol-enhanced P450 gene pool contributes to cotton bollworm tolerance to a pyrethroid insecticide. *Mol Ecol* 2012;**21**:4371–85.

12. Darband SG, Kaviani M, Yousefi B *et al.* Quercetin: a functional dietary flavonoid with potential chemo-preventive properties in colorectal cancer. *J Cell Physiol* 2018;**233**:6544–60.

13. Kuipers E, Dam A, Held N *et al.* Quercetin lowers plasma triglycerides acompanied by white adipose tissue browning in diet-induced obese mice. *Int J Mol Sci* 2018;**19**:1786.

14. Sharma A, Kashyap D, Sak K *et al.* Therapeutic charm of quercetin and its derivatives: a review of research and patents. *Pharm Pat Anal* 2018;**7**:15–32.

15. Ben Salem I, Boussabbeh M, Graiet I *et al.* Quercetin protects HCT116 cells from Dichlorvos-induced oxidative stress and apoptosis. *Cell Stress Chaperones* 2015;**21**:179–86.

16. Sadiq A, Khan S, Shah SMH. Larvicidal, insecticidal, brine shrimp cytotoxicity and anti-oxidant activities of *Diospyros kaki* (L.) reported from Pakistan. *Pak J Pharm Sci* 2015;**28**:1239–43.

17. Santos PC, Santos VHM, Mecina GF *et al.* Insecticidal activity of *Tagetes* sp. on *Sitophilus zeamais* mots. *Int J Environ Agric Res* 2016;**2**:31–8.

18. Santos PC, Santos VHM, Mecina GF *et al.* Phytotoxicity of *Tagetes erecta* L. and *Tagetes patula* L. on plant germination and growth. *S Afr J Bot* 2015;**100**:114–21.

19. Li S, Cao C, Shi H *et al.* Effect of quercetin against mixture of four organophosphate pesticides induced nephrotoxicity in rats. *Xenobiotica* 2015;**46**:225–33.

20. Ghosh S, Tiwari SS, Srivastava S *et al.* Acaricidal properties of *Ricinus communis* leaf extracts against organophosphate and pyrethroids resistant *Rhipicephalus (Boophilus) microplus*. *Vet Parasitol* 2013;**192**:259–67.

21. Ramos S, Sultatos L. Flavonoid-induced alterations in cytochrome P450-dependent biotransformation of the organophosphorus insecticide parathion in the mouse. *Toxicology* 1998;**131**:155–67.

22. Liu D, Yuan Y, Li M *et al.* Effects of dietary quercetin on performance and cytochrome P450 expression of the cotton bollworm, *Helicoverpa armigera*. *Bull Entomol Res* 2015;**105**:771–7.

23. Pilipenko N, Ropstad E, Halsne R *et al.* Effect of naringenin, quercetin, and sesamin on xenobiotica-metabolizing CYP1A and CYP3A in mice offspring after maternal exposure to persistent organic pollutants. *Biomed Res Int* 2017;**2017**:1–8.

24. Elbarbry F, Ung A, Abdelkawy K. Studying the inhibitory effect of quercetin and thymoquinone on human cytochrome p450 enzyme activities. *Pharmacogn Mag* 2018;**13**:S895.

25. Mao W, Schuler MA, Berenbaum MR. Disruption of quercetin metabolism by fungicide affects energy production in honey bees (*Apis mellifera*). *Proc Natl Acad Sci* 2017;**114**:2538–43.

26. Li P, Callery PS, Gan L-S *et al.* Esterase inhibition by grapefruit juice flavonoids leading to a new drug interaction. *Drug Metab Dispos* 2007;**35**:1203–8.

27. Sehgal SA, Khattak NA, Mir A. Structural, phylogenetic and docking studies of D-amino acid oxidase activator (DAOA), a candidate schizophrenia gene. *Theor Biol Med Model* 2013;**10**:3.

28. Guerrini A, Gianni S. Chemical fingerprinting of medicinal and aromatic plant extracts: HPTLC bioautographic assays as preliminary research tool to match chemical and biological properties. *J Med Aromat Plants* 2014;**3**:1000e152.

29. Sehgal SA, Kanwal S, Tahir RA *et al.* In silico elucidation of potential drug target sites of the thumb index fold protein, Wnt-8b. *Trop J Pharm Res* 2018;**17**:491–7.

30. Sehgal S, Tahir R, Shafique S *et al.* Molecular modeling and docking analysis of CYP1A1 associated with head and neck cancer to explore its binding regions. *J Theor Comput Sci* 2014;**1**:2.

31. Tahir RA, Sehgal SA, Khattak NA *et al.* Tumor necrosis factor receptor superfamily 10B (TNFRSF10B): an insight from structure modeling to virtual screening for designing drug against head and neck cancer. *Theor Biol Med Model* 2013;**10**:38.

32. Sehgal SA, Mannan S, Kanwal S *et al.* Adaptive evolution and elucidating the potential inhibitor against schizophrenia to target DAOA (G72) isoforms. *Drug Des Devel Ther* 2015;**9**:3471–80.

33. Sehgal SA. Pharmacoinformatics and molecular docking studies reveal potential novel proline dehydrogenase (PRODH) compounds for schizophrenia inhibition. *Med Chem Res* 2017;**26**:314–26.

34. Sehgal SA, Hassan M, Rashid S. Pharmacoinformatics elucidation of potential drug targets against migraine to target ion channel protein KCNK18. *Drug Des Devel Ther* 2014;**8**:571–81.

35. Sehgal SA. Pharmacoinformatics, adaptive evolution, and elucidation of six novel compounds for schizophrenia treatment by targeting DAOA (G72) isoforms. *Biomed Res Int* 2017;**2017**:1–19.

36. Xu C, Ding Y, Ni J *et al.* Tumor-targeted docetaxel-loaded hyaluronic acid-quercetin polymeric micelles with p-gp inhibitory property for hepatic cancer therapy. *RSC Adv* 2016;**6**:27542–56.

37. Sehgal SA, Mirza AH, Tahir RA *et al. Quick Guideline for Computational Drug Design.* Sharjah, U.A.E: Bentham Science Publishers, 2018.

38. Malik K, Chaudhri AK. Electrophoretic analysis of *Tribolium castaneum* after combined bioassay with cinnamon (*Cinnamomum aromaticum*), turmeric (*Curcuma longa*) and onion seed powder (*Nigella sativa*). *BEPLS* 2016;**5**:37–41.

39. The_UniProt_Consortium. UniProt: a worldwide hub of protein knowledge. *Nucleic Acids Res* 2018;**47**:D506–15.

40. Burley SK, Berman HM, Kleywegt GJ *et al.* Protein Data Bank (PDB): The Single Global Macromolecular Structure Archive. In: Wlodawer A, Dauter Z, Jaskolski M (Editors) *Protein Crystallography: Methods and Protocols.* New York: Springer, 2017, pp. 627–641.

41. Šali A, Blundell TL. Comparative protein modelling by satisfaction of spatial restraints. *J Mol Biol* 1993;**234**:779–815.

42. Källberg M, Wang H, Wang S *et al.* Template-based protein structure modeling using the RaptorX web server. *Nat Protoc* 2012;**7**:1511.

43. Schwede T. SWISS-MODEL: an automated protein homology-modeling server. *Nucleic Acids Res* 2003;**31**:3381–5.

44. Fernandez-Fuentes N, Madrid-Aliste CJ, Rai BK *et al.* M4T: a comparative protein structure modeling server. *Nucleic Acids Res* 2007;**35**:W363–8.

45. Zhang Y. I-TASSER server for protein 3D structure prediction. *BMC Bioinformatics* 2008;**9**:40.

46. Kelley LA, Mezulis S, Yates CM *et al.* The Phyre2 web portal for protein modeling, prediction and analysis. *Nat Protoc* 2015;**10**:845.

47. Pettersen EF, Goddard TD, Huang CC *et al.* UCSF chimera—a visualization system for exploratory research and analysis. *J Comput Chem* 2004;**25**:1605–12.

48. Cheatham TE III, Cieplak P, Kollman PA. A modified version of the Cornell *et al.* force field with improved sugar pucker phases and helical repeat. *J Biomol Struct Dyn* 1999;**16**:845–62.

49. Colovos C, Yeates T. ERRAT: an empirical atom-based method for validating protein structures. *Protein Sci* 1993;**2**:1511–9.

50. Laskowski RA, MacArthur MW, Moss DS *et al*. PROCHECK: a program to check the stereochemical quality of protein structures. *J Appl Crystallogr* 1993;**26**:283–91.

51. Eisenberg D, Lüthy R, Bowie JU. *Methods in Enzymology*, Vol. **277**. Elsevier, 1997, 396–404.

52. Chen VB, Arendall WB, Headd JJ *et al*. MolProbity: all-atom structure validation for macromolecular crystallography. *Acta Crystallogr D Biol Crystallogr* 2010;**66**:12–21.

53. Emsley P, Lohkamp B, Scott WG *et al*. Features and development of coot. *Acta Crystallogr Sect D* 2010;**66**:486–501.

54. Bowie J, Luthy R, Eisenberg D. A method to identify protein sequences that fold into a known three-dimensional structure. *Science* 1991;**253**:164–70.

55. Lüthy R, Bowie JU, Eisenberg D. Assessment of protein models with three-dimensional profiles. *Nature* 1992;**356**:83–5.

56. Jones G, Willett P, Glen RC *et al*. Development and validation of a genetic algorithm for flexible docking. *J Mol Biol* 1997;**267**:727–48.

57. Goodsell DS, Morris GM, Olson AJ. Automated docking of flexible ligands: applications of AutoDock. *J Mol Recognit* 1996;**9**:1–5.

58. Wallace AC, Laskowski RA, Thornton JM. LIGPLOT: a program to generate schematic diagrams of protein-ligand interactions. *Protein Eng Des Sel* 1995;**8**:127–34.

59. Ray GB, Cook JW. Molecular modeling of heme proteins using MOE: bio-inorganic and structure-function activity for undergraduates. *Biochem Mol Biol Educ* 2005;**33**:194–201.

60. Trott O, Olson AJ. AutoDock Vina: improving the speed and accuracy of docking with a new scoring function, efficient optimization, and multithreading. *J Comput Chem* 2010;**31**:455–61.

61. Mills N. ChemDraw Ultra 10.0 CambridgeSoft, 100 CambridgePark Drive, Cambridge, MA 02140. www.cambridgesoft.com. Commercial price: 1910 for download, 2150 for CD-ROM; academic price: 710 for download, 800 for CD-ROM. *Aust Dent J* 2006;**41**:13649–50.

62. Bergmann DJ, Hooper AB. The primary structure of cytochrome P460 of *Nitrosomonas europaea*: presence of a c-heme binding motif. *FEBS Lett* 1994;**353**:324–6.

63. Rose RL, Goh D, Thompson DM *et al*. Cytochrome P450 (CYP) 9A1 in *Heliothis virescens*: the first member of a new CYP family. *Insect Biochem Mol Biol* 1997;**27**:605–15.

64. Guo Z, Sevrioukova IF, Denisov IG *et al*. Heme binding biguanides target cytochrome P450-dependent cancer cell mitochondria. *Cell Chem Biol* 2017;**24**:1259–1275.e1256.

65. Skerratt SE, de Groot MJ, Phillips C. Discovery of a novel binding pocket for CYP 2C9 inhibitors: crystallography, pharmacophore modelling and inhibitor SAR. *Med Chem Commun* 2016;**7**:813–9.

66. Jadhav DR, Mallikarjuna N, Rathore A *et al*. Effect of some flavonoids on survival and development of *Helicoverpa armigera* (Hübner) and *Spodoptera litura* (fab) (Lepidoptera: Noctuidae). *Asian J Agric Sci* 2012;**4**:298–307.

67. Dong J, Zhang Q, Cui Q *et al*. Flavonoids and naphthoflavonoids: wider roles in the modulation of cytochrome P450 family 1 enzymes. *Chem Med Chem* 2016;**11**:2102–18.

68. Aboshi T, Ishida M, Matsushita K *et al*. Stage-specific quercetin sulfation in the gut of *Mythimna separata* larvae (Lepidoptera: Noctuidae). *Biosci Biotechnol Biochem* 2014;**78**:38–40.

69. Costa LG, Garrick JM, Roquè PJ *et al*. Mechanisms of neuroprotection by quercetin: counteracting oxidative stress and more. *Oxidative Med Cell Longev* 2016;**2016**:1–10.

70. Forte L, Torricelli P, Boanini E *et al*. Antioxidant and bone repair properties of quercetin-functionalized hydroxyapatite: an in vitro osteoblast–osteoclast–endothelial cell co-culture study. *Acta Biomater* 2016;**32**:298–308.

71. Napal GND, Defagó MT, Valladares GR *et al*. Response of *Epilachna paenulata* to two flavonoids, pinocembrin and quercetin, in a comparative study. *J Chem Ecol* 2010;**36**:898–904.

72. Mesbah H, Saad A, Mourad A *et al*. Joint action of quercetin with four insecticides on the cotton leaf-worm larvae, *Spodoptera littoralis* Boisd.(Lepidoptera: Noctuidae) in Egypt. *Commun Agric Appl Biol Sci* 2007;**72**:445–57.

73. Mansour MH, Dimetry NZ. Effect of three plant growth regulators on the immature stages of the cotton leaf worm *Spodoptera littoralis* (Boisd.) (Lep., Noctuidae). *Z Angew Entomol* 2009;**80**:88–93.

74. Wang Z, Zhao Z, Cheng X *et al*. Conifer flavonoid compounds inhibit detoxification enzymes and synergize insecticides. *Pestic Biochem Physiol* 2016;**127**:1–7.

75. Nelson DR. Progress in tracing the evolutionary paths of cytochrome P450. *Biochim Biophys Acta* 2011;**1814**:14–8.

76. Berge J, Feyereisen R, Amichot M. Cytochrome P450 monooxygenases and insecticide resistance in insects. *Philos Trans R Soc B Biol Sci* 1998;**353**:1701–5.

77. Chan HH, Wajidi MFF, Zairi J. Molecular cloning and xenobiotic induction of seven novel cytochrome P450 monooxygenases in *Aedes albopictus*. *J Insect Sci* 2014;**14**.

78. Zhu F, Parthasarathy R, Bai H *et al*. A brain-specific cytochrome P450 responsible for the majority of deltamethrin resistance in the QTC279 strain of *Tribolium castaneum*. *Proc Natl Acad Sci* 2010;**107**:8557–62.

79. Almira Correia M, Sinclair PR, De Matteis F. Cytochrome P450 regulation: the interplay between its heme and apoprotein moieties in synthesis, assembly, repair, and disposal. *Drug Metab Rev* 2011;**43**:1–26.

80. Minakuchi C, Ishii F, Washidu Y *et al*. Expressional and functional analysis of CYP15A1, a juvenile hormone epoxidase, in the red flour beetle *Tribolium castaneum*. *J Insect Physiol* 2015;**80**:61–70.